

NEXT GENERATION ACTIVE TWIST HELICOPTER ROTOR BLADE - SIMULATED RESULTS VALIDATED BY EXPERIMENTAL INVESTIGATION

Steffen Kalow

Bram van de Kamp

Ralf Keimer

Johannes Riemenschneider

Steffen.Kalow@dlr.deBram.vandekamp@dlr.deRalf.Keimer@dlr.deJohannes.Riemenschneider@dlr.de

Scientist

Scientist

Scientist

Acting Head of the Department Adaptronics

Institute of Composite Structures and Adaptive Systems

German Aerospace Center (DLR)

Braunschweig, Germany

Abstract

Vibration and noise are omnipresent in a helicopter environment and therefore their reduction is an important goal in helicopter research. Actuators embedded into the skin of a helicopter rotor blade can produce a twist, which influences the propagation of the air turbulence. Hence, vibration and noise levels can be reduced significantly. An important issue during operation of these rotor blades is the centrifugal load which affects the actuators and can cause a failure [3]. Based on the German Aerospace Center (DLR) project STAR (Smart Twisting Active Rotor), the design of an active twist rotor blade has been adapted, such that the loads in the actuator system can be significantly reduced and furthermore distributed evenly. This paper builds on previous publications [1-5]. After a brief summary of the improved blade design and the manufacturing process, this publication mainly refers to the determination of the structural blade properties of the first manufactured rotor blades. Specifically, torsional stiffness, lead lag bending stiffness as well as chordwise elastic axis position and twist performance are determined. These results are compared to the simulation findings and especially analyzed with regard to blade-to-blade differences. The experimental setup and also the measuring method are explained in detail.

1. BACKGROUND AND MOTIVATION

The basic principle of individual blade control and its benefits for an improved aerodynamic behavior has been shown in many different studies [10]. The goals of helicopter research are vibration and noise reduction as well as performance improvement. Active twist rotors can actively contribute to this. Embedded into the skin of a rotor blade, piezo ceramic actuators are able to twist the entire rotor blade and thus influence the propagation of air vortexes.

For several years the German Aerospace Center investigated this technology and built several model rotor blades. A history of these activities can be found in [1-9]. In 2013 DLR was prepared for a wind tunnel test with a four-bladed, fully instrumented rotor within the project STAR (Smart Twisting Active Rotor). But shortly before the end of the pre-test [5] fatigue problems occurred and the wind tunnel test had to be canceled. Since then, DLR has been researching the causes of failure and creating a new rotor blade design that increases the durability. The results, presented for the first time at AHS 2016 [3], showed that the

integration of the actuators is a huge challenge, because the actuators are subject to considerable loads due to the centrifugal force, which are the main reason for the actuator failures.

Based on these findings the actuator and the rotor blade design were completely revised so that the loads in the actuator system are significantly reduced and furthermore distributed evenly. In addition to a new actuator design, the use of carbon fiber composite for the spar and additional straps near to the trailing edge increase the durability of the new generation of active twist rotor blades, which is the basis for a specific and efficient research of the active twist technology.

2. DESIGN CHANGES

In the beginning of the design phase the new model rotor blade it is important to define all mandatory boundary conditions. These boundary conditions will have influence on the approach to the multidisciplinary design process [4]. Mainly the internal structure and the material selection are decisive for the active twist, the strength, stability

und dynamic properties. In order to meet all requirements and find an improved design, an iterative process is necessary.

2.1 SIMULATION MODEL

The design is based on the experiences of the previous blade generations and results from the simulated blade properties. However, many relevant features must be taken into account within the design process. For that a lot of different design variations have been simulated and their results analyzed [3]. Therefore a tool called SaMaRA (Structural Modeling and Rotor Analysis) was developed [4]. It consists of a parametric finite element model for passive or active rotor blades and the numeric analysis code to determine the blades structural properties. SaMaRA was developed to meet the partially contradictory requirements (e.g. different requirements for bending and torsional stiffness or axes positions of rotor blades) in the context of structural optimization. This rotor blade simulation tool uses the ANSYS software and is based on the Ansys Parametric Design Language (APDL). The simulation environment is based on the calculation of individual 2D cross-sections.

2.2 IMPROVED BLADE DESIGN

As already mentioned a lot of different design variations have been simulated and analyzed. Some of the simulated design approaches were for example:

- using other materials for certain components (e.g. CFRP spar)
- altered fiber angle in the skin
- additional unidirectional layers of GFRP or CFRP in skin
- implementing unidirectional fibers in the skin at the trailing edge
- reducing the stiffness of the balance weight
- reinforce layers behind actuator
- different actuator design configurations
- different cable positions

The evaluation of all design approaches finally led to the design shown in figure 1. Furthermore, the comparison of the previous design and the new STAR design is presented. The main design changes are the use of CFRP for the spar and also placing additional CFRP straps near to the trailing edge. Compared to the previous design, the simulation results of the improved blade design show a significant reduction of the strains

under pure centrifugal loads, especially at the trailing edge [1]. Furthermore, the strains distribution over the chord length is much better due to the proximity of the center of gravity and the tension axis.

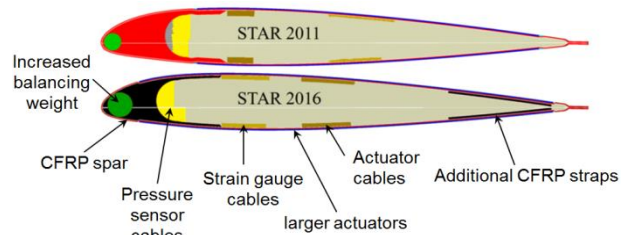


Figure 1: comparison of previous and new rotor design

Table 1 gives a brief overview about the simulated blade properties of both designs.

Table 1. Comparison of calculated blade parameters at $r/R=0.25$

Characteristics	Design 2011	Design 2016
Lead lag bending stiffness	7194 Nm ²	26500 Nm ²
Flap bending stiffness	174 Nm ²	280 Nm ²
Torsional stiffness	169 Nm ²	185 Nm ²
Tensile stiffness	13500 kN	29500 kN
Center of gravity	25.9 %chord	25.5 %chord
Tension Center	19.2 %chord	25.5 %chord
Mass per length	1.32 kg/m	1.47 kg/m
Twist (-500V to 700V)	5.4°	5.7°

The goal is to build a complete four-bladed rotor. Here, the reproducibility is another important requirement. All DLR active rotor blades are handmade and therefore unique. To ensure that all blades have the same characteristics, each blade will have an identical structure, although they will be instrumented differently. In the less equipped rotor blades sensors will be replaced by dummies and sensor cables will remain. Since the first set of STAR blades showed different properties between the blades, this approach is chosen to minimize any deviations. Furthermore, an identical blade design contributes to a more standardized manufacturing process, which also adds to the objective of similar blades. To get an impression of the highly detailed models which were generated, figure 2 shows the skin with integrated actuators (dark brown for GFRP, lighter brown for the actuators) and the inner design with spar and straps made of carbon fiber (grey). Furthermore the pressure sensors (light brown) next to the cable tree in green and in a very dark grey the balancing weights at the leading edge are shown. The requirement for equality between the blades is very important and has a decisive influence on the design of the blades.

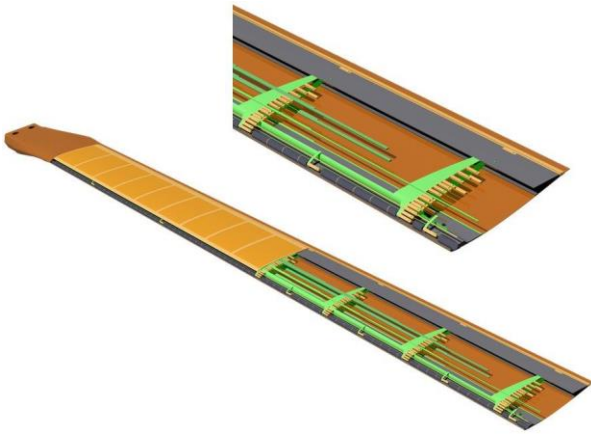


Figure 2: Detailed rotor blade design

3 BLADE MANUFACTURING

A first prototype of the newly designed rotor blade has been built in 2017. Since the results of the laboratory tests and whirl tower tests [2] were very promising, the decision was made to build 5 new blades, a complete 4-bladed-rotor and an additional fifth blade as backup. These blades purposes are to prove the functionality of the active twist technology in a wind tunnel test campaign. At the time of publication, three of the five planned rotor blades have already been manufactured. A more detailed manufacturing description can be found in [1]. The next section contains only a selected overview.

The 5 blades differ only in there instrumentation. All blades have a total of 25 strain gauges each to measure the torsion, flap and lag bending movement (9 for torsion, 9 for flap and 7 for lag). However, the pressure sensor distribution is different. Common to all are 10 individual pressure sensors on the upper side and the lower side on the leading edge of the rotor blade. In addition to these, blade 1 and blade 2 have further pressure sensors distributed over 4 dedicated radial profile sections. To ensure that the rotor blades properties are approximately the same, the remaining blades get dummy masses at these positions. A total of up to 225 pressure sensors are installed in the blades.

Due to the increasing complexity with increasing number of pressure sensors, it was decided to start with the production of blade 5 (the replacement blade) and finally manufacture blade 1 and 2 last.

The manufacturing process of highly instrumented rotor blades is very challenging. Due to the small size of the scaled blades, the manufacturing has

to be very precise and allows only very little deviation in comparison to the CAD design. Especially the properties regarding stiffness and center of gravity have to meet the calculated ones. As already mentioned, the reproducibility is also a big issue that has to be solved. In STAR there were partially large deviations between the individual blades, which are partly attributable to the thermal shrinkage, amounts of adhesive or different instrumentation. Due to the new design a combination of glass fiber components and carbon fiber components is used, which has not been done in active blades at DLR before. This adds further challenges to the manufacturing process. The requirement to build 5 blades with similar properties has a very high priority. Among other things, this raises the need to have the same work steps carried out in all blades by a consistent manufacturing team, since different ways of working can have a significant impact on the blade properties (e.g., mass and stiffness distribution). This procedure enables much better results in terms of flutter stability or blade comparability. Therefore, a detailed manufacturing schedule was developed, including specified manufacturing steps in accordance to a standardized process. Furthermore, the integrity of the actuators must be ensured at all times until the completion of the manufacturing process. Numerous preliminary tests and maximum care in dealing with the sensitive actuators are a prerequisite for this.

4 EXPERIMENTAL EVALUATION OF STRUCTURAL BLADE PROPERTIES

In the following, the test rig for determining the elastic properties of the blade as well as the used measuring methods are described. The blade properties of the prototype blade and the comparison with the old STAR blades have already been presented in [2]. Therefore, the subject of this chapter is mainly the comparison of the blade properties of the new blades with each other. They are also compared with the results of the prototype blade and the simulation. The test setup for previously tested rotor blades and the test setup described here are almost identical. The following properties regarding the airfoil region are measured and compared:

- Torsional stiffness
- Flap bending stiffness
- Chordwise position of the elastic axis
- Active twist angle with actuators.

4.1 Measurement of torsional and flap bending stiffness as well as the elastic axis chordwise position

Torsional and flap bending stiffness as well as the elastic axis chordwise position are determined for the airfoil region between its initial radial position and the end of the actuator area. Segments with modifications of the cross section due to implemented pressure sensors and contacts are considered to be of small radial extension compared to the blade length. Consequently, the structural properties are determined based on the assumption that the blades possess a uniform cross section design over the regarded region. Accordingly, the obtained structural properties represent averaged values.

4.1.1 Test setup

The first three properties are determined in one test setup. The blade is clamped at the bolts directly at the blade root and hold in an upward position as it is exemplarily shown for blade 5 in figure 3. Additionally, it is fixed at the beginning of the airfoil region using an airfoil shaped clamp (figure 4). In order to improve clamping and thus to increase the accuracy of the measurement, a massive clamp (figure 4 right) is used in comparison to earlier measurements (figure 4 left).

The blade is then loaded like a single side supported beam by an external force at the end of the actuator area within the airfoil region. Therefore, another clamp is mounted at the end of the actuator area near to the blade tip. The clamp is extended in chordwise direction such that it could be used as a lever for force application. The leading edge of the profile is defined as zero on the lever.

The force is applied perpendicular to the radial blade axis and also radial to the profile chord near the blade tip by a string. The string is pulled by an excenter rotating with 0.3 HZ to avoid creeping effects of the glass fiber composite material of the rotor blade. At the other end the string is attached to a load cell, to relate the displacements to their corresponding forces. The point of application of the force can be changed along the lever. The blade deformation is measured with a photogrammetric system for the old STAR blades and with a laser profile scanner for the new STAR blades. Both systems can determine the in plane movement of the clamp perpendicular to the spanwise direction. A schematic of the test setup is shown in figure 5.



Figure 3: Test rig with rotor blade 5



Figure 4: left: Test rig with old clamp;
right: Test rig with new massive clamp

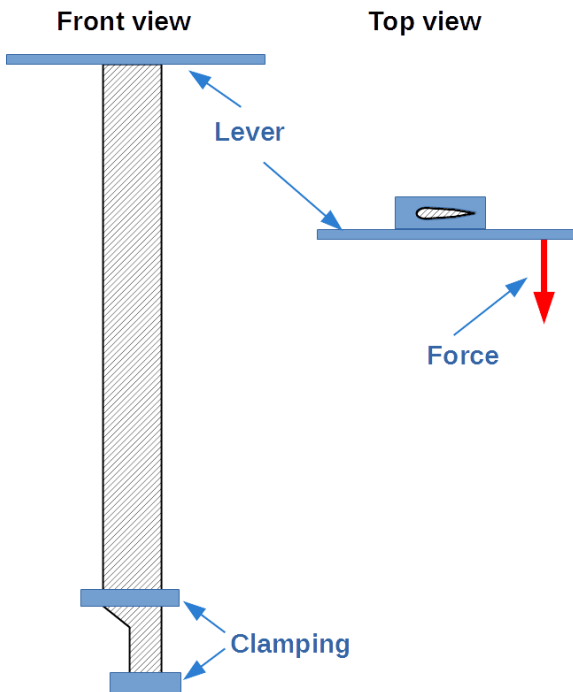


Figure 5: Test setup schematic

4.1.2 Calculating stiffness and elastic axis from plane deformation and force

In order to calculate the desired properties from the in plane movements of the clamp the assumption can be made that any force F applied to the cross section is equivalent to the same force applied to the elastic axis combined with a moment $F \cdot d$ as shown in figure 6.

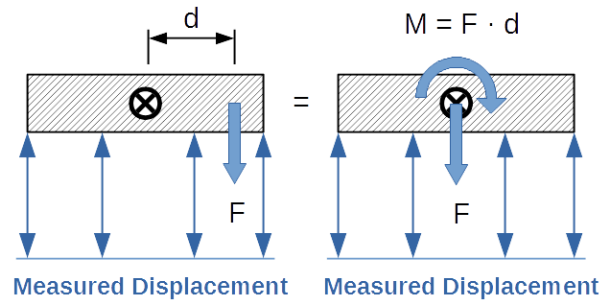


Figure 6: Measuring and calculation schematic

Accordingly resulting displacements w in profile thickness direction with varying force application points along the clamp and lever are measured. The experiment is performed several times and the results are then averaged.

The position of the elastic axis and thus length d is unknown. Therefore the data is used to calculate an angle of rotation. By interpolation the position with no rotational angle and thus a zero moment M could be determined, shown in figure 7.

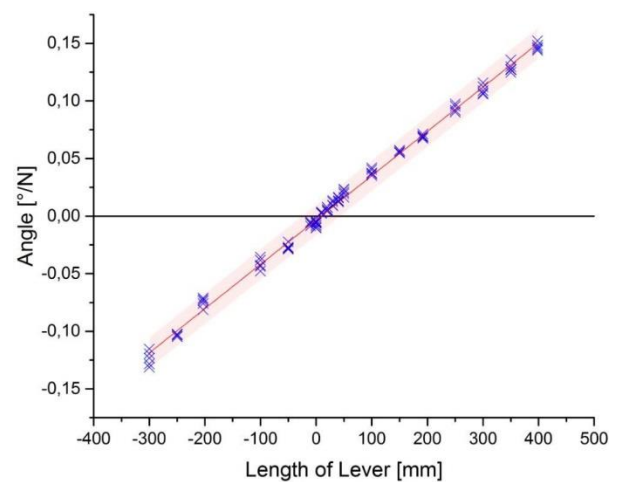


Figure 7: Lever displacements

As a zero moment M can only be obtained when d is zero. The elastic axis of the rotor blade is the point in figure 7 where the linear regression of angle and length of lever cross the $0 = N$ -axis. Knowing the position of the elastic axis, the applied moment M_T is derived for every single measurement and then related to the rotational angle ϑ_l and the length l between the clamping positions, resulting in the torsional stiffness GI_T of the rotor blade:

$$(1) \quad GI_T = \frac{M_T l}{\vartheta_l}$$

Likewise the displacement w is derived at the position of the elastic axis for every single measurement and correlated to the force F and the length l between the clamping positions, resulting in the flap bending stiffness EI_{flap} :

$$(2) \quad EI_{flap} = \frac{l^3 F}{3 w}$$

4.1.3 Results and Discussion

In previous measurements, the described procedure was carried out exclusively in the flap-up direction and the axis positions and stiffnesses were determined from this. However, it has been shown that the pre-twist of the blades ($4^\circ/m$) has an influence on the measurement results. The pre-twist inevitably leads to a bending-torsion coupling when a force is applied in the direction of flapping. This leads to different deflections and thus to inaccurate results with a deviation of up to 10%. Therefore the determination for both flap-up and flap-down has been carried out since blade 5. The resulting axial positions and stiffnesses are then averaged to increase accuracy. Another point has not yet been conclusively clarified. Currently, the results are determined by introducing the load perpendicular to the profile at the blade tip. The pre-twist of the blade and the associated bending-torsion coupling can lead to different results if the load is introduced in a different radial profile.

At the time of publication, three of the five planned rotor blades have already been manufactured. It should be noted that at this time the results had unfortunately not yet been fully evaluated. Therefore, the parts presented here are still preliminary results. Blade 4 and blade 5 are compared with the prototype blade. Furthermore, the results are compared with the simulation. The results to the old STAR blades can be found in [1, 2, 5].

Using the test set-up described in the previous section, the position of the elastic axis can be determined. figure 8 shows the comparison of elastic axis positions. Since the prototype blade has only been measured flap-up and is no longer available, the results are only partially comparable or contain deviations of up to 10%. The simulated axis position is at about 18% of chord length. Blade 5 is in close range to this result. The elastic axis position of blade 4 is slightly below.

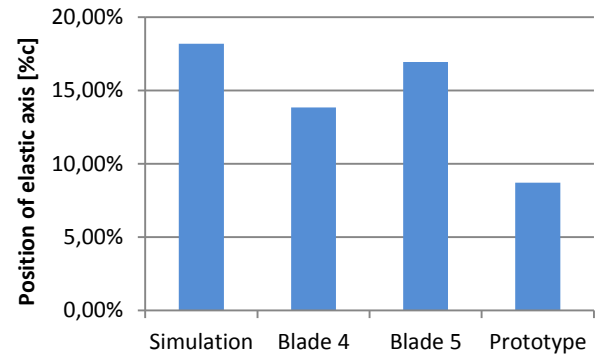


Figure 8: Comparison of elastic axis position

The resulting differences suggest that the accuracy of the measurement method is reaching its limits here. Due to the geometry the measured deflections in flap direction are much higher than in torsion while a force is applied as described near to the blade tip. Therefore, the determination of the torsion angle is very difficult, since it is not possible to initiate a pure moment. Nevertheless, there are differences due to measurement inaccuracies, e.g. the assumption that the introduced forces are approximately the same or that the lever arm can be determined with sufficient accuracy. Even a deviation of few millimeters, e.g. at the load application point, can lead to a significant change in the results. Furthermore, the effects of temperature influences on the measurement results are unclear. Although no concrete investigations have been done that fluctuations in room temperature have a visible influence on the test, but it should be taken into account of error analysis, as for example the creep behaviour under static load due to the glass fiber composite material. In this case, an eccentric load is used in this experiment instead of a static load to avoid creeping effects.

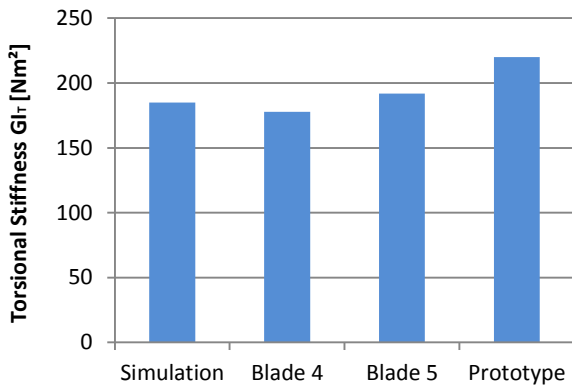


Figure 9: Comparison of torsional stiffness

A comparison of torsional and flap bending stiffness is given in figure 9 and figure 10. It can be seen, that due to the incorrect results of the elastic axis the magnitude of the torsional stiffness and also the flap bending stiffness of the prototype blade is slightly higher than the others. However, it is important to consider the stiffnesses of blade 4 and blade 5.

For the torsional stiffness both are very close to the simulation results. A closer look at the values shows, that there are also differences between blade 4 and 5 due to the measurement setup, but they are within the possible standard deviations, so they match the simulation very well.

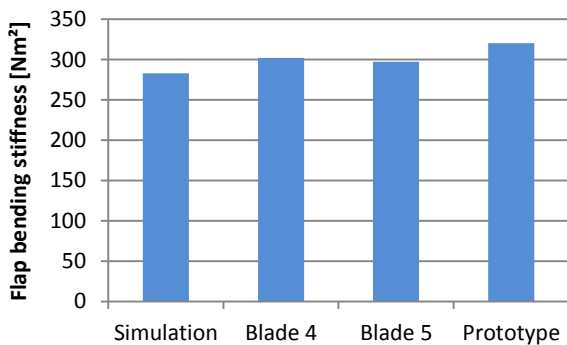


Figure 10: Comparison of flap bending stiffness

The flap bending stiffness of both blades is almost the same, but slightly different from the simulation. This can be due to different assumptions of the boundary conditions in the simulation as well as to different material characteristics. For example, for the tungsten-resin combination in the balancing weight as well as for the bonded cable harnesses, smeared material characteristics had to be approximated. Nevertheless, the results are very promising, as the differences between the blades are very small, which is very important for the further progress of the DLR project.

4.2 Measurement of active twist angle

Lastly the active twist angle is measured. Therefore the rotor blade is solely clamped at the bolts. The actuators are controlled by a harmonic excitation of 600V and a simultaneous offset of 400V. This results in a control range of -200V to 1000V. The selected frequency is 0.01 Hz, which corresponds to a quasi-static excitation. As can be seen in figure 11 the active twist of all blades is slightly lower than expected, but in any case sufficient to achieve the project objectives (0-4/rev = 4°pp and 5+6/rev = 2°pp)

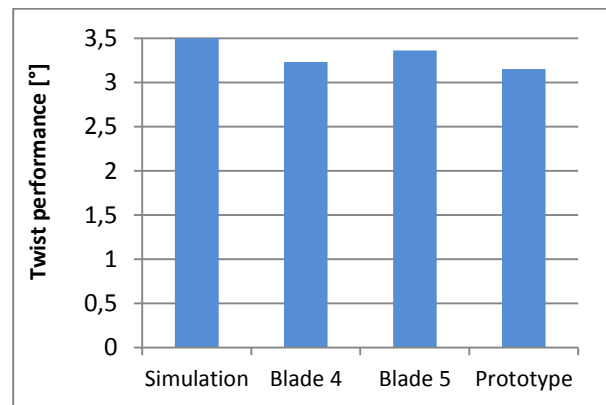


Figure 11: Comparison of active twist

5 OPTICAL MEASUREMENTS

To validate the position of the elastic axis determined experimentally in 4.3, a further procedure was utilised. Using a high-resolution camera system, it was possible to prove that the determined elastic axis position is approximately correct. This measurement method was initially tested for blade 5 (figure 12).

The ARAMIS system consists of 2 cameras with a resolution of 12 megapixels. After prior calibration of the system using certified calibration objects to a defined measurement coordinate system, 3D displacements on the rotor blade can be recorded in a certain range.

In order to capture the entire rotor blade, 10 individual measurements are recorded and then transferred to a common coordinate system. The results can then be combined and evaluated qualitatively. For these tests, a defined load successively is applied at the determined elastic axis as well as at the leading edge and trailing edge of the rotor blade in flap direction. figure 13 shows the displacements out of the plane as a result of the respective load introduction. It can be

seen that the load introduction at the elastic axis does not lead to any torsion (figure 13b). For the other two load cases, different deflections can be recognized at the leading edge and the trailing edge of the blade, which is equivalent to a torsion (figure 13a,c).



Figure 12: Optical measurement of blade 5

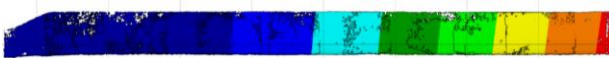


Figure 13a: Displacements due to load introduction at the leading edge

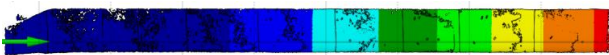


Figure 13b: Displacements due to load introduction at the determined elastic axis position



Figure 13c: Displacements due to load introduction at the trailing edge

Thus it could be shown for the first time that it is possible to combine the evaluations of individual sections and obtain an analysis of the entire rotor blade. Unfortunately, the resolution of the camera system is not sufficient to determine the quality of the elastic axis. Deviations in the range of a few millimeters in chord direction cannot currently be resolved. However, in the future this method could also be used to display a continuous curvature along the bending line.

6 CONCLUSION AND OUTLOOK

The actuators embedded in an active twist rotor blade are exposed to considerable loads due to the high centrifugal force. Based on the DLR project STAR [5], a rotor blade design was completely revised. In addition to various material and structural adaptations, this includes a revised actuator design. The experimental results from numerous tests with a prototype [2] confirm the clear reduction of strains under centrifugal load and are very promising with regard to a significantly better durability of the rotor blades. Based on the positive results, DLR decided to produce a complete blade set with 4 blades and a spare blade as the next generation of rotor blades. Hereby, the similarity of the individual rotor blades and their properties is an important goal. In order to achieve this and due to the high requirements and the limited installation space, a detailed manufacturing concept is essential. At the time of publication, three rotor blades have already been manufactured, but not yet completely measured in the laboratory. All results shown here can therefore be considered as preliminary.

The experimental results confirm the simulations in most aspects. The bending and torsional stiffness as well as the twist performance of blades 4 and 5 are very close to each other and as such are very promising with regard to the requirement for the very similar structural properties between all 5 blades. Measurement deviations, especially in the determination of the chordwise elastic axis position, result mainly from the fact that the measured angles and deflections are very small. Small discrepancies can lead to large deviations. Whereas the introduced force is assumed to be determined sufficiently well. The question how to reference the results has not yet been conclusively clarified. Currently, the results are determined by introducing the load orthogonally to the profile at the blade tip. Due to the pre-twist of the blade and the associated bending torsion coupling, deviating results may be obtained if the load is introduced in a different

radial profile. The results should therefore initially be assumed as a first approximation.

It could also be shown that it is possible to roughly validate the position of the elastic axis by combining several optically measured individual evaluations. In the future, this system can be used to investigate a continuous curvature along the blade radius.

By the end of 2019, all 5 rotor blades will most likely be manufactured. After a laboratory evaluation of the structural blade properties, each individual blade is to be qualified in the whirl tower and then the complete rotor will be prepared for the wind tunnel. Testing in the wind tunnel is scheduled to take place in 2021. A newly formed consortium with international partners will support the campaign, including further simulations and validations.

REFERENCES

- [1] Kalow, S., van de Kamp, B., Balzarek, C. und Riemenschneider, J., "*Manufacturing of a next generation active twist helicopter rotor blade and experimental results of functionality test*", American Helicopter Society 74th Annual Forum Proceedings, Phoenix, Arizona, USA, May 2018.
- [2] Kalow, S., van de Kamp, B., Keimer, R. and Riemenschneider, J., "*Experimental investigation and validation of structural properties of a new design for active twist rotor blades*", European Rotorcraft Forum 43th Annual Forum Proceedings, Milan, Italy, September 2017.
- [3] Kalow, S., Opitz, S., Riemenschneider, J. and Hoffmann, F., "*Results of a parametric study to adapt structural properties and strain distribution of active twist blades*", American Helicopter Society 72th Annual Forum Proceedings, West Palm Beach, Florida, USA, May 2016.
- [4] van de Kamp, B., Kalow, S., Riemenschneider, J., Bartels, R., and Mainz, H., "*Multidisciplinary design chain for model rotor blades*", International Council of Aeronautical Sciences, Daejeon, Südkorea, September 2016
- [5] Hoffmann, F., Schneider, O., van der Wall, B.G., Keimer, R., Kalow, S., Bauknecht, A., Ewers, B., Pengel, K. and Feenstra, G., "*STAR hovering test - proof of functionality and representative results*", 40th European Rotorcraft Forum, number 10-B in Conference Proceedings online, pages 1–19, September 2014.
- [6] Riemenschneider, J., Keimer, R. and Kalow, S., "*Experimental bench testing of an active twist rotor*", European Rotorcraft Forum 39th Annual Forum Proceedings, Moscow, Russia, September 2013.
- [7] Monner, H.P., Riemenschneider, J., Opitz, S. and Schulz, M., "*Development of active twist rotors at the German Aerospace Center (DLR)*", 16th AIAA/ASME/AHS Adaptive Structures Conference, San Diego, USA, April 2011.
- [8] Monner, H.P., Opitz, S., Riemenschneider, J. and Wierach, P., "*Evolution of active twist rotor designs at DLR*", 49th AIAA/ASME/ASCE/AHS/ASC Structures, Structural Dynamics, and Materials Conference, Schaumburg, Illinois, April 2008.
- [9] Wierach, P., Riemenschneider, J., Opitz, S. and Hoffmann, F., "*Experimental investigation of an active twist model rotor blade, under centrifugal loads*", European Rotorcraft Forum 33th Annual Forum Proceedings, Kazan, Russia, September 2007.
- [10] Maucher, C.K., Grohmann, B.A. and Junker, P., "*Review of adaptive helicopter rotor blade actuation concepts*", Adaptronic Congress, Göttingen, Germany, May 2006.

COPYRIGHT STATEMENT

The authors confirm that they, and/or their company or organization, hold copyright on all of the original material included in this paper. The authors also confirm that they have obtained permission, from the copyright holder of any third party material included in this paper, to publish it as part of their paper. The authors confirm that they give permission, or have obtained permission from the copyright holder of this paper, for the publication and distribution of this paper as part of the ERF proceedings or as individual offprints from the proceedings and for inclusion in a freely accessible web-based repository.